ADVANCED SCIENCE Open Access
www.advancedscience.com

Construction of New Active Sites: Cu Substitution Enabled Surface Frustrated Lewis Pairs over Calcium Hydroxyapatite for CO_2 Hydrogenation

Jiuli Guo, Yan Liang, Rui Song, Joel Y. Y. Loh, Nazir P. Kherani, Wu Wang, Christian Kübel, Ying Dai,* Lu Wang,* and Geoffrey A. Ozin**

Calcium hydroxyphosphate, $Ca_{10}(PO_4)_6(OH)_2$, is commonly known as hydroxyapatite (HAP). The acidic calcium and basic phosphate/hydroxide sites in HAP can be modified via isomorphous substitution of calcium and/or hydroxide ions to enable a cornucopia of catalyzed reactions. Herein, isomorphic substitution of Ca^{2+} ions by Cu^{2+} ions especially at very low levels of exchange created new analogs of molecular surface frustrated Lewis pairs (SFLPs) in $Cu_xCa_{10-x}(PO_4)_6(OH)_2$, thereby boosting its performance metrics in heterogeneous CO_2 photocatalytic hydrogenation. In situ Fourier transform infrared spectroscopy characterization and density functional theory calculations provided fundamental insights into the catalytically active SFLPs defined as proximal Lewis acidic Cu^{2+} and Lewis basic OH^-. The photocatalytic pathway proceeds through a formate reaction intermediate, which is generated by the reaction of CO_2 with heterolytically dissociated H_2 on the SFLPs. Given the wealth of information thus uncovered, it is highly likely that this work will spur the further development of similar classes of materials, leading to the advancement and, ultimately, large-scale application of photocatalytic CO_2 reduction technologies.

1. Introduction

In recent years, excessive CO_2 emissions caused by fossil fuel combustion and automobile exhaust emissions have seriously disturbed the natural carbon cycle and exacerbated global warming. Gas-phase photocatalytic CO_2 reduction has attracted global attention; it aims to reduce CO_2 into commodity chemicals and fuels exemplified by CO, CH_4, HCOOH, CH_3OH, and C_{2+} by using resource-rich, economical, clean, and renewable solar energy.[1] Surface frustrated Lewis pairs (SFLPs) can activate H_2 and CO_2 molecules due to their ability to form a highly activated structural space for adsorbed molecules. As a result, SFLPs have been implicated in gas-phase photocatalytic CO_2 hydrogenation to CO, CH_4, and CH_3OH.[2]

To amplify, the SFLPs sites (i.e., In—OH···In) in $In_2O_{3-x}(OH)_y$ serve to

Dr. J. Guo
School of Chemistry and Chemical Engineering
Anyang Normal University
Anyang, Henan 455000, P. R. China
E-mail: guojiuli@aynu.edu.cn

Dr. J. Guo, Dr. R. Song, Dr. J. Y. Y. Loh, Prof. N. P. Kherani, Prof. G. A. Ozin
Solar Fuels Group
Centre for Inorganic and Polymeric Nanomaterials
Department of Chemistry
University of Toronto
Toronto, M5S 3H6, Canada
E-mail: g.ozin@utoronto.ca

Dr. Y. Liang, Prof. Y. Dai
School of Physics
State Key Laboratory of Crystal Materials
Shandong University
Jinan, Shandong 250100, P. R. China
E-mail: daiy60@sdu.edu.cn

The ORCID identification number(s) for the author(s) of this article can be found under https://doi.org/10.1002/advs.202101382

DOI: 10.1002/advs.202101382

Dr. J. Y. Y. Loh, Prof. N. P. Kherani
Department of Electrical and Computer Engineering
Department of Materials Science and Engineering
University of Toronto
Toronto, M5S 3E4, Canada

Dr. W. Wang, Dr. C. Kübel
Karlsruhe Institute of Technology (KIT)
Institute of Nanotechnology (INT)
and Karlsruhe Nano Micro Facility (KNMF)
Hermann-von-Helmholtz-Platz 1, Building 640,
Eggenstein-Leopoldshafen 76344, Germany

Dr. C. Kübel
Technical University Darmstadt (TUDa)
Department of Materials & Earth Sciences
Alarich-Weiss-Straße 2, Darmstadt 64287, Germany

Prof. L. Wang
School of Science and Engineering
The Chinese University of Hong Kong (Shenzhen)
Guangdong 518172, P. R. China
E-mail: lwang@cuhk.edu.cn

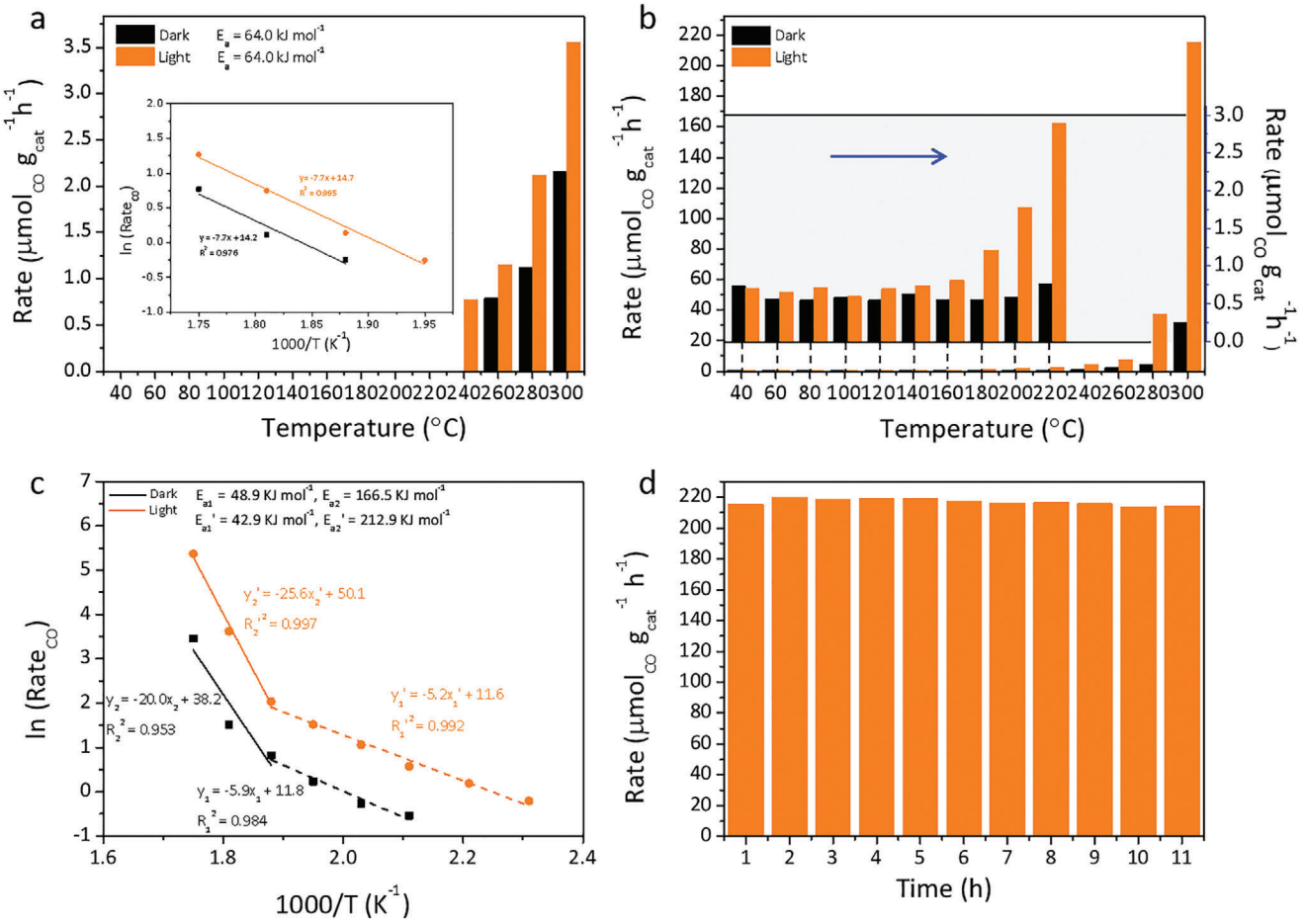

Figure 1. Photocatalytic performance of 0 and 0.5 mol% Cu-HAP in the flow reactor. CO rate of a) 0 and b) 0.5 mol% Cu-HAP in the flow reactor under dark and light conditions. Arrhenius plots for CO production rates of 0 mol% Cu-HAP are shown inset of Figure 1a. c) Arrhenius plots for CO production rates of 0.5 mol% Cu-HAP. d) Catalytic stability results for 0.5 mol% Cu-HAP in a flow reactor over 11 h at 300 °C under light conditions. Reaction conditions for flow measurements: atmospheric pressure, light intensity of ≈2.0 W cm^{-2}, H_2/CO_2 ratio = 1:1 with flow rate of 2 sccm.

capture and convert CO_2 to either CO or CH_3OH.[2b,3] As well, oxygen vacancies were introduced in $CoGeO_2(OH)_2$ using photogenerated holes to oxidize the hydroxyl groups of the lattice, where SFLPs involving unsaturated coordinated surface cobalt sites and adjacent hydroxyl catalyze the formation of CH_4 from CO_2 and H_2O.[4] Additionally, through isomorphous substitution of In^{3+} in $In_2O_{3-x}(OH)_y$ or In_2O_3 with Bi^{3+}, the reactivity of the SFLPs themselves in $Bi_zIn_{2-z}O_{3-x}(OH)_y$ or $Bi_xIn_{2-x}O_3$ can be tailored to advantage in heterogeneous CO_2 photocatalytic hydrogenation.[5]

Recently, we have discovered Cu^{2+} ions substitute for Ca^{2+} into the HAP lattice and hydrated Cu^{2+} species therein migrate and deposit to form CuO at the surface for high levels of exchange Cu-HAP.[6] Notably, Cu^{2+}/PO_4^{3-} SFLPs at high levels of exchange Cu-HAP were found to greatly enhance CO_2 reduction to CO driven photothermally.[6]

To understand if the Cu^{2+} in HAP structure has any relevance in the reaction, it became apparent that low levels of exchange (0 and 0.5 mol%) Cu-HAP might be advantageous to avoid CuO in flow CO_2 conversion to products. Amazingly, these results revealed a CO production rate of 215 μmol g_{cat}^{-1} h^{-1} with no CH_4 being detected for 0.5 mol% Cu-HAP, which is around 61 orders photoactivity enhancement of the reverse water gas shift (RWGS) reaction compared to the pristine 0 mol% Cu-HAP. What surprised us, even more, was the new Cu^{2+}/OH^- SFLPs in 0.5 mol% Cu-HAP, composed of coordinately unsaturated copper sites, adjacent to an oxygen vacancy and a hydroxide group, enable the heterolysis of H_2 and reaction with CO_2 to form CO through a formate reaction intermediate driven photocatalytically.

2. Results and Discussion

The synthesis of 0 and 0.5 mol% Cu-HAP is accomplished by the co-precipitation method. 0.5 mol% Cu-HAP displayed the very similar powder X-ray diffraction (PXRD) pattern of hexagonal (space group $P6_3/m$) HAP but a small shift to lower 2θ diffraction angles relative to those of 0 mol% Cu-HAP (Figure S1, Supporting Information), which signals the substitution of the larger ionic radius Ca^{2+} (1.0 Å) by smaller Cu^{2+} (0.73 Å).[5] This conclusion is further supported by representative scanning transmission electron microscopy imaging in combination with energy-dispersive X-ray spectroscopy images of 0.5 mol%

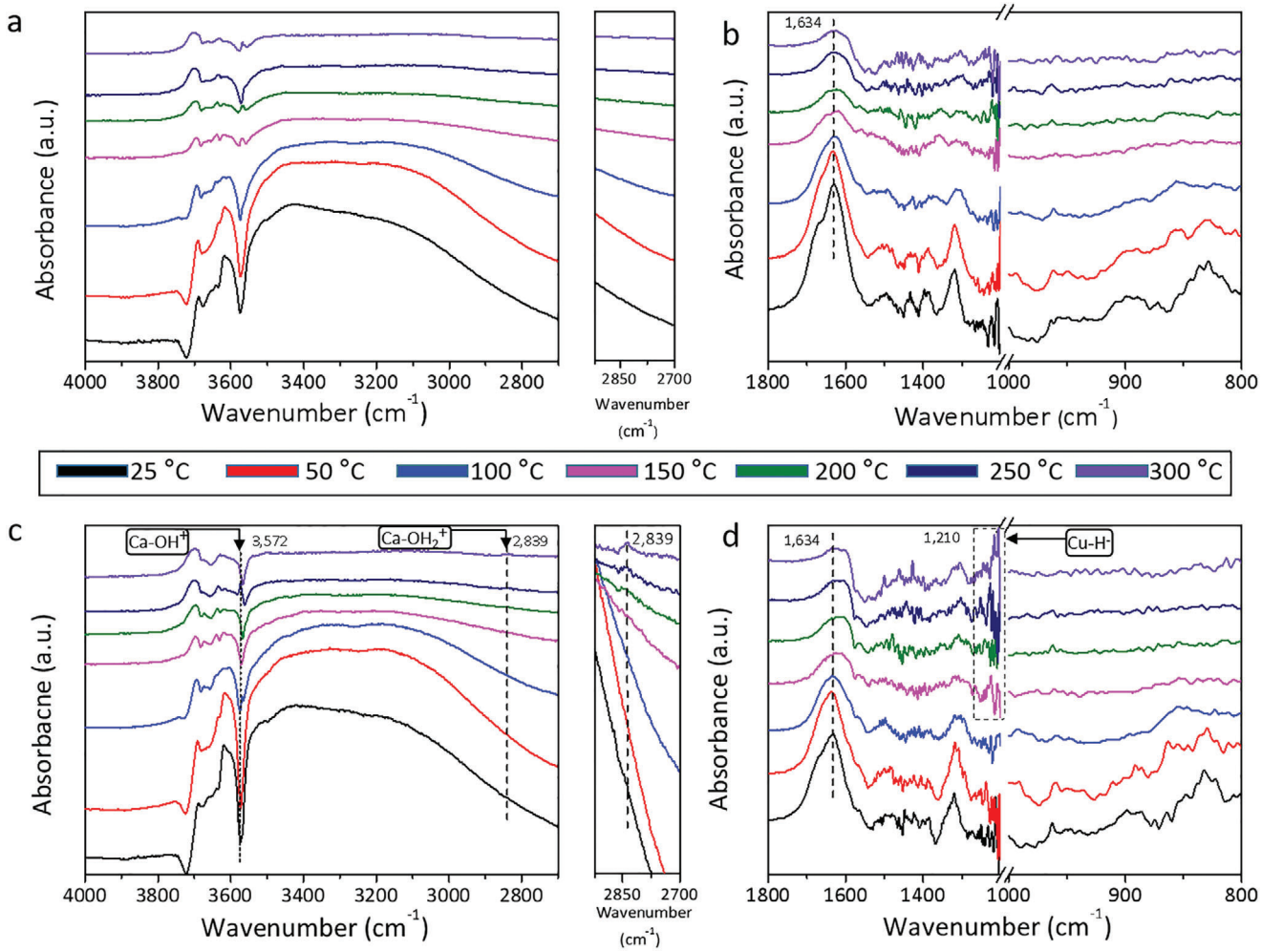

Figure 2. DRIFTS results for 0 and 0.5 mol% Cu-HAP. DRIFTS spectra obtained during H_2 (1 sccm H_2, 19 sccm He) adsorption on a,b) 0 and c,d) 0.5 mol% Cu-HAP after 30 min at each temperature.

Cu-HAP nanocrystals, where no metallic Cu or CuO_x nanoparticles were observed despite a significant Cu loading (Figure S2, Supporting Information). Furthermore, electron paramagnetic resonance (EPR) signals from 0.5 mol% Cu-HAP were recorded and confirm the Cu^{2+} sites in the HAP lattice (Figure S3, Supporting Information).[7]

Samples were tested at different temperatures in the flow reactor with and without light irradiation. As shown in **Figure 1**a,b, 0.5 mol% Cu-HAP was more active than 0 mol% Cu-HAP to catalyze RWGS reaction, $CO_2 + H_2 \rightarrow CO + H_2O$ towards the sole production CO detected (confirmed by $^{13}CO_2$ isotope labeling in Figure S4, Supporting Information). Notably, 0.5 mol% Cu-HAP showed higher CO rate of 215 $\mu mol_{CO}\ g_{cat}^{-1}\ h^{-1}$ at 300 °C under light than 0 mol% Cu-HAP by around 61 orders of magnitude. The linear Arrhenius behavior for 0 mol% Cu-HAP suggests that a single catalytic process occurs within the temperature range of the study under both dark and light (inset of Figure 1a). Surprisingly, the corresponding Arrhenius plots for 0.5 mol% Cu-HAP showed two-stage linear plots with activation energies of 48.9 kJ mol^{-1} (low temperature, 200–260 °C) and 166.5 kJ mol^{-1} (high temperature, 260–300 °C) under dark, and 42.9 kJ mol^{-1} (low temperature, 160–260 °C) and 212.9 kJ mol^{-1} (high temperature, 260–300 °C) with light (Figure 1c), indicating two different reaction pathways.[8] The control test revealed no activity in blank reactor with quartz wool at 300 °C and light illumination.

An 11-h stability of 0.5 mol% Cu-HAP was investigated in the capillary flow reactor at 300 °C with light (Figure 1d), and showed a decrease in production rate of only 0.5%. It is noteworthy that the PXRD pattern of the spent 0.5 mol% Cu-HAP indicated the intact hydroxyapatite (HAP) lattice and no copper nanocrystal was observed (Figure S5), which was further supported by that no visible change for its light blue color.

Operando Diffuse Reflectance Infrared Fourier Transform Spectroscopy (DRIFTS) is a powerful technique for observing surface species participating in catalytic reactions under real-world conditions. The DRIFTS method was therefore applied to study the RWGS reaction photocatalyzed by 0 and 0.5 mol% Cu-HAP, the goal being to identify fingerprint vibrational modes diagnostic of adsorbed reactants and intermediates that exist as a function of temperature and time.

Operando DRIFTS experiments were performed to gain an insight into the RWGS reaction catalyzed by 0 and 0.5 mol%

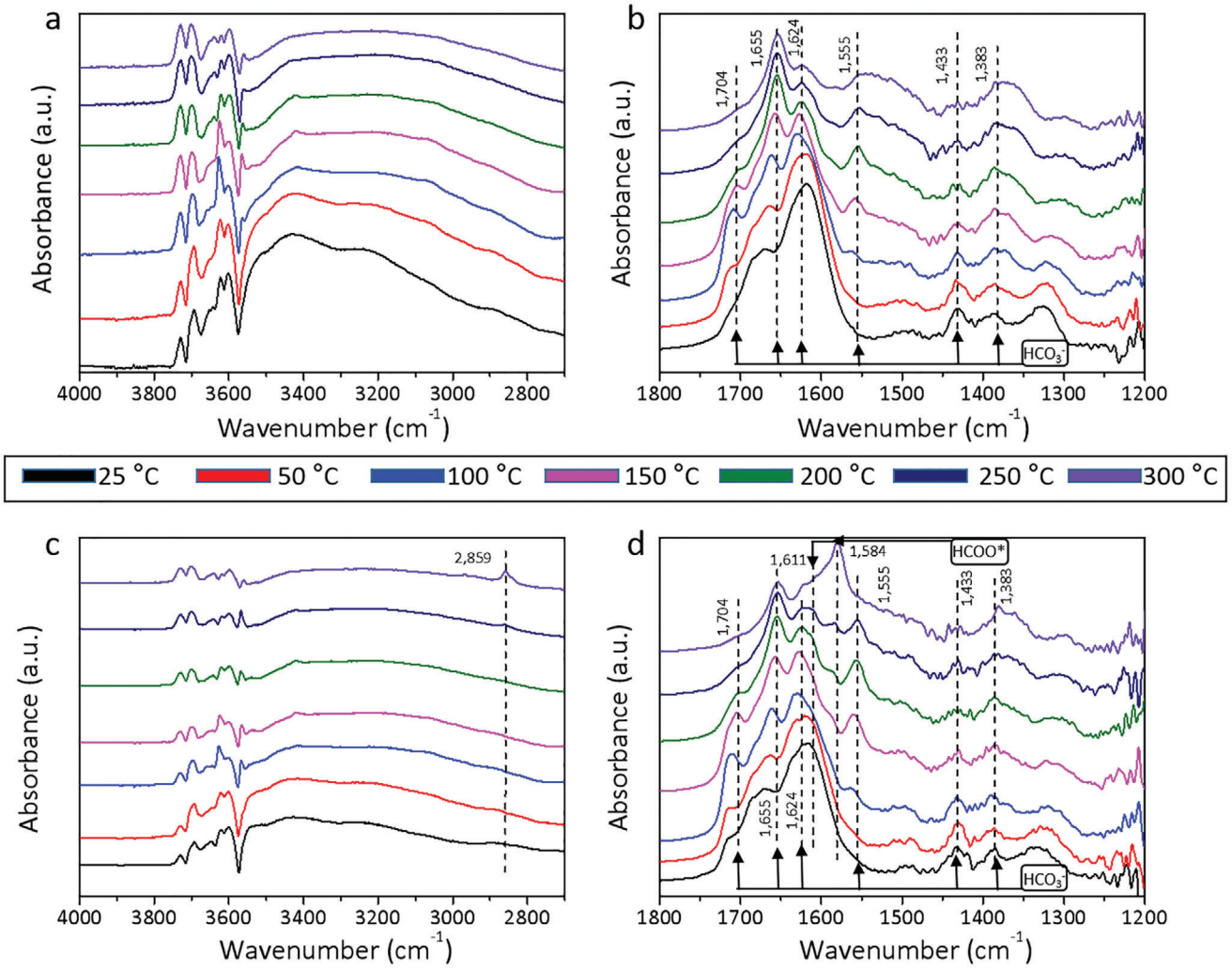

Figure 3. DRIFTS studies of 0 and 0.5 mol% Cu-HAP. H_2 and CO_2 (1 sccm H_2, 1 sccm CO_2, 18 sccm He) adsorption spectra of a,b) 0 and c,d) 0.5 mol% Cu-HAP after 30 min at different temperatures.

Cu-HAP. One type involves exposing the catalysts to H_2 (**Figure 2**), these experiments were conducted as a function of temperature and time to provide information on adsorbed surface hydrogen species. The surprising observation revealed that the H_2 molecule reacts with 0.5 mol% Cu-HAP to produce new vibrational modes in the hydroxyl and metal hydride stretching and deformation regions with increased temperature, in which the 0 mol% Cu-HAP showed nothing. In detail, the peaks at 1210 and 2839 cm^{-1} can be assigned to Cu-H^- and Ca-OH_2^+, respectively.[2c,9] For peak located at 3,572 cm^{-1}, could be attributed to the protonated calcium oxide species ($Ca\text{-}OH^+$),[2c] and further evidence stems from their appearance of 250 °C and disappearance of 300 °C (Figure S6, Supporting Information). Furthermore, the decreased peak intensity under He confirmed the presence of Cu-H^- and Ca-OH_2^+ (Figure S7, Supporting Information). The peak at 1,634 cm^{-1} can be ascribed to adsorbed water.[9b] No HPO_4^{2-} peaks were observed at 3235, 1235, 831 cm^{-1} at high temperatures, indicating PO_4^{3-} was not involved in the hydrogen activation on SFLPs.[6,10] These results indicate that H_2 is undergoing heterolysis on proximal Lewis acidic Cu^{2+} and Lewis basic OH^- SFLPs to form CuH^-/Ca-OH_2^+ surface sites.

Further operando DRIFT study was conducted and explored the reaction of catalysts with H_2-CO_2 mixtures under flow conditions after aforementioned H_2 absorption, probed as a function of temperature and time (**Figure 3**). Significantly, CuH^- and Ca-OH_2^+ peaks were replaced by those of reaction intermediates gradually changed from bicarbonate to formate with increasing temperature, consistent with the observations of two-stage linear plots in Arrhenius plots of 0.5 mol% Cu-HAP (Figure 1c). The peaks located at 1704, 1655, 1624, 1555, 1433, and 1383 cm^{-1} can be attributed to bicarbonate intermediates.[6,9b,11] For peaks at 2859, 1611, and 1584 cm^{-1}, correspond to vibrational modes of formate species.[6,11,12] The decrease of CO_2 peak (3600–3800 cm^{-1}) intensity reflected an enhanced CO_2 activation over 0.5 mol% Cu-HAP with Cu^{2+} substitution.[2c,6] The growth of intense vibrational modes in hydroxyl stretching and deformation region also confirmed the enhanced CO_2 activation, as well as the higher H_2 adsorption capacity (Figure S8, Supporting Information).

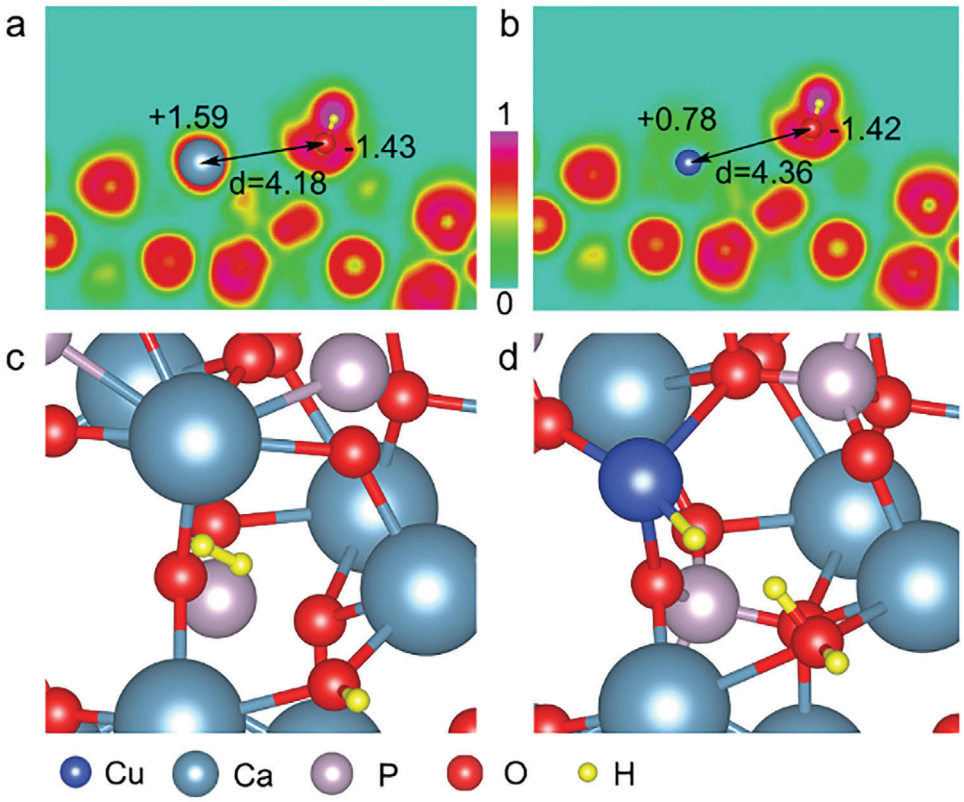

Figure 4. SFLPs on a) 0 mol% Cu-HAP (211) and b) 0.5 mol% Cu-HAP (211), where the background denotes the electron localization. Configurations of H_2 adsorption at the c) Ca—OH···Ca SFLPs site in 0 mol% Cu-HAP (211) and d) Ca—OH···Cu SFLPs site in 0.5 mol% Cu-HAP (211).

X-ray photoelectron spectroscopy (XPS) spectra were acquired during exposure of 0.5 mol% Cu-HAP to 1:1 ratio of CO_2/H_2 atmosphere at 300 °C under light (Figure S9, Supporting Information). A positive shift for O 1s ionization potentials of the hydroxyl flags the H_2 heterolysis on the surface of 0.5 mol% Cu-HAP, along with the generation of additional hydroxides and protonation.[3b] Concurrently, the Cu 2p XPS peak slightly shifted to lower energy due to the formation of hydrides by H_2 heterolysis, resulting in the low effective nuclear charge at coordinately unsaturated copper Lewis acid sites.[3b] Furthermore, surface Cu atomic percentages in 0.5 mol% Cu-HAP before and after photocatalytic reaction (1 h) did not show a significant change, which were determined to be 0.07% and 0.06% via XPS analysis, respectively (Figure S9b, Supporting Information). Solid-state ^1H MAS-NMR spectra of 0.5 mol% Cu-HAP treated before and after exposing to H_2 at atmospheric pressure and 300 °C provide additional support for H_2 heterolysis on SFLPs Ca—OH···Cu sites (Figure S10, Supporting Information). Two new chemical shifts around 8.23 and 12.33 ppm can be assigned as Cu-H^- and Ca-OH_2^+ sites, respectively.[3b,13]

DFT calculations were carried out to further reveal the promotion effect of Cu^{2+} substitution on HAP. The HAP (211) facet has been chosen for the calculation and explanation for its low average surface energy (Table S1, Supporting Information). Then, we studied the possible SFLPs site in HAP (211) with/without Cu substitution. Intrinsic OH group and metal atom at the (211) surface of HAP act as Lewis basic and Lewis acidic sites, respectively. After surface relaxation and leave out pairs where the distances are too close or too far, we screen out one possible SFLPs in pure and single-site Cu substituted HAP (211). O and Ca pair include atomic local charges of +1.59 e and −1.43 e in pure HAP (211), and +0.78 e, −1.42 e for O atom and the near Cu atom are involved in single-site Cu substituted HAP (211). The distances between the active O atom and Ca/Cu atom are 4.18 and 4.36 Å, respectively (**Figure 4**a,b). These results indicated surface OH group and Ca/Cu are suitable for SFLPs.[5b] On the other hand, to study the origin of the observed improvement of CO_2 hydrogenation, the SFLPs-mediated rate-determine step (H_2 dissociation) is considered (Figure 4c,d). It is found that Cu substitution induced SFLPs to dissociate H_2 much easier, while in pristine HAP (211), H_2 tends to maintain as a single molecule (0 K). This behavior could result from the atomic electronic configuration where the charge localization near Cu is less favorable relative to that around the Ca (see Figure 4a,b). This can be the main factor that in turn influences the bonding between H atom and intermediate products.[5b,12a]

Another point worth mentioning is that the valence band positions of 0 and 0.5 mol% Cu-HAP were determined to be −15.84 eV and −15.33 eV (vs vacuum) by ultraviolet photoelectron spectroscopy (UPS), and conduction band positions were located at −13.08 and −12.55 eV (vs vacuum), respectively (Figures S11 and S12). Notably, photoluminescence results for 0 and 0.5 mol% Cu-HAP show an efficient charge transfer at the interface with Cu substitution (Figure S13, Supporting Information). One can surmise that photogenerated electrons and holes would relax to mid-gap Lewis-acidic Cu^{2+} and Lewis-basic OH^- sites of

SFLPs, enhancing its Lewis acidity and Lewis basicity and thereby contribute to significantly increased catalytic rates of 0.5 mol% Cu-HAP.[1b,2c,5b,11,12a]

Collecting together all of the results of this study, intended to define how Cu^{2+} in HAP structure relate to the gas-phase heterogeneous (photo)catalytic hydrogenation of CO_2, for low levels of replacement x of Ca^{2+} by Cu^{2+}, one can draw the reaction pathway for the production of CO by heterogeneous hydrogenation of gaseous CO_2 on 0.5 mol% Cu-HAP. At low temperatures (25–≈250 °C), surface oxygen vacancies could act as active sites leading to bicarbonate intermediates for CO_2 hydrogenation to produce CO and H_2O.[2c,14] While at high temperatures (≈250–300 °C), H_2 heterolytically dissociated on SFLPs Ca—OH···Cu to form Ca—OH_2^+···CuH^-, subsequent reaction of the formate intermediates with protons of Ca—OH_2^+ form CO and H_2O, thereby completing the RWGS catalytic cycle (Figure S14, Supporting Information). This is consistent with the higher production of CO even at dark conditions for 0.5 mol% Cu-HAP (31.5 μmol g_{cat}^{-1} h^{-1}) than 0 mol% Cu-HAP (2.2 μmol g_{cat}^{-1} h^{-1}).

3. Conclusion

In conclusion, complementary DRIFTS, UPS, in situ XPS, ^{1}H MAS NMR, and DFT calculations provided insight into a new kind of SFLPs in low Cu^{2+} exchange $Cu_xCa_{10-x}(PO_4)_6(OH)_2$, the identities of surface intermediates and details of photocatalytic reaction pathways. A formate reaction intermediate is identified, which is generated by the reaction of CO_2 with heterolytically dissociated H_2 on Ca—OH···Cu lattice pairs to form Ca—OH_2^+···CuH^-. This represents a new class of SFLP for gas-phase heterogeneous (photo)catalytic hydrogenation of CO_2. Opportunities for additional modifications to the Lewis acidic and basic properties of the HAP are possible using different cations, which bodes well for tuning the activity and selectivity of the catalyst to produce a variety of products from CO_2.

Supporting Information

Supporting Information is available from the Wiley Online Library or from the author.

Acknowledgements

G.A.O. is a Government of Canada Research Chair in Materials Chemistry and Nanochemistry. Financial support for this work was provided by the Ontario Ministry of Research Innovation (MRI); Ministry of Economic Development, Employment and Infrastructure (MEDI); Ministry of the Environment and Climate Change (MOECC); Ministry of Research Innovation, Low Carbon Innovation Fund (LCIF); Connaught Innovation Fund; Connaught Global Challenge Fund; and the Natural Sciences and Engineering Research Council of Canada (NSERC). L.W. would like to acknowledge the financial support from the University Development Fund (UDF01001721) and the Program for Guangdong Introducing Innovative and Entrepreneurial Teams (2019ZT08L101). J.G. acknowledges funding from the Anyang Normal University Cultivation Fund (AYNUKPY-2019-11); University Innovation Fund (S202010479011).

Conflict of Interest

The authors declare no conflict of interest.

Data Availability Statement

The data that support the findings of this study are available from the corresponding author upon reasonable request.

Keywords

copper, gas-phase reactions, hydroxyapatite, surface chemistry, surface frustrated Lewis pair

Received: April 5, 2021
Revised: May 3, 2021
Published online:

[1] a) Y. Li, D. Hui, Y. Sun, Y. Wang, Z. Wu, C. Wang, J. Zhao, *Nat. Commun.* **2021**, *12*, 123; b) T. Yan, N. Li, L. Wang, Q. Liu, A. Jelle, L. Wang, Y. Xu, Y. Liang, Y. Dai, B. Huang, J. You, G. A. Ozin, *Energy Environ. Sci.* **2020**, *13*, 3054; c) M. Wang, M. Shen, X. Jin, J. Tian, M. Li, Y. Zhou, L. Zhang, Y. Li, J. Shi, *ACS Catal.* **2019**, *9*, 4573. d) E. T. Kho, T. H. Tan, E. Lovell, R. J. Wong, J. Scott, R. Amal, *Green Energy Environ.* **2017**, *2*, 204; e) U. Ulmer, T. Dingle, P. N. Duchesne, R. H. Morris, A. Tavasoli, T. Wood, G. A. Ozin, *Nat. Commun.* **2019**, *10*, 3169; f) A. Wagner, C. D. Sahm, E. Reisner, *Nat. Catal.* **2020**, *3*, 775; g) H. Wang, W. Zhang, L. Lu, D. Liu, T. Li, S. Yan, S. Zhao, Z. Zou, *Appl. Catal., B* **2021**, *283*, 119639.

[2] a) Y. Ma, S. Zhang, C. -R. Chang, Z. -Q. Huang, J. C. Ho, Y. Qu, *Chem. Soc. Rev.* **2018**, *47*, 5541; b) L. B. Hoch, T. E. Wood, P. G. O'Brien, K. Liao, L. M. Reyes, C. A. Mims, G. A. Ozin, *Adv. Sci.* **2014**, *1*, 1400013; c) L. Wang, Y. Dong, T. Yan, Z. Hu, A. A. Jelle, D. M. Meira, P. N. Duchesne, J. Y. Y. Loh, C. Qiu, E. E. Storey, Y. Xu, W. Sun, M. Ghoussoub, N. P. Kherani, A. S. Helmy, G. A. Ozin, *Nat. Commun.* **2020**, *11*, 2432.

[3] a) L. Wang, M. Ghoussoub, H. Wang, Y. Shao, W. Sun, A. A. Tountas, T. E. Wood, H. Li, J. Y. Y. Loh, Y. Dong, M. Xia, Y. Li, S. Wang, J. Jia, C. Qiu, C. Qian, N. P. Kherani, L. He, X. Zhang, G. A. Ozin, *Joule* **2018**, *2*, 1; b) L. Wang, T. Yan, R. Song, W. Sun, Y. Dong, J. Guo, Z. Zhang, X. Wang, G. A. Ozin, *Angew. Chem., Int. Ed.* **2019**, *58*, 9501.

[4] X. Wang, L. Lu, B. Wang, Z. Xu, Z. Xin, S. Yan, Z. Geng, Z. Zou, *Adv. Funct. Mater.* **2018**, *28*, 1804191.

[5] a) Y. Dong, K. K. Ghuman, R. Popescu, P. N. Duchesne, W. Zhou, J. Y. Y. Loh, A. A. Jelle, J. Jia, D. Wang, X. Mu, C. Kübel, L. Wang, L. He, M. Ghoussoub, Q. Wang, T. E. Wood, L. M. Reyes, P. Zhang, N. P. Kherani, C. V. Singh, G. A. Ozin, *Adv. Sci.* **2018**, *5*, 1700732; b) T. Yan, N. Li, L. Wang, W. Ran, P. N. Duchesne, L. Wan, N. T. Nguyen, L. Wang, M. Xia, G. A. Ozin, *Nat. Commun.* **2020**, *11*, 6095.

[6] J. Guo, P. N. Duchesne, L. Wang, R. Song, M. Xia, U. Ulmer, W. Sun, Y. Dong, J. Y. Y. Loh, N. P. Kherani, J. Du, B. Zhu, W. Huang, S. Zhang, G. A. Ozin, *ACS Catal.* **2020**, *10*, 13668.

[7] a) G. Li, N. M. Dimitrijevic, L. Chen, T. Rajh, K. A. Gray, *J. Phys. Chem. C* **2008**, *112*, 19040; b) I. Ardelean, S. Cora, D. Rusu, *Phys. B* **2008**, *403*, 3682.

[8] F. Chang, Y. Guan, X. Chang, J. Guo, P. Wang, W. Gao, G. Wu, J. Zheng, X. Li, P. Chen, *J. Am. Chem. Soc.* **2018**, *140*, 14799.

[9] a) C. M. Lousada, R. M. F. Fernandes, N. V. Tarakina, I. L. Sorokab, *Dalton Trans.* **2017**, *46*, 6533; b) L. Wan, Q. Zhou, X. Wang, T. E. Wood, L. Wang, P. N. Duchesne, J. Guo, X. Yan, M. Xia, Y. F. Li, A. A. Jelle, U. Ulmer, J. Jia, T. Li, W. Sun, G. A. Ozin, *Nat. Catal.* **2019**, *2*, 889.

[10] a) M. I. Domínguez, F. Romero-Sarria, M. A. Centeno, J. A. Odriozola, *Appl. Catal. B* **2009**, *87*, 245; b) C. Sun, D. Xue, *CrystEngComm* **2013**, *15*, 10445.

[11] C.-S. Chen, C. S. Budi, H.-C. Wu, D. Saikia, H.-M. Kao, *ACS Catal.* **2017**, *7*, 8367.

[12] a) T. Yan, L. Wang, Y. Liang, M. Makaremi, T. E. Wood, Y. Dai, B. Huang, A. A. Jelle, Y. Dong, G. A. Ozin, *Nat. Commun.* **2019**, *10*, 2521; b) X. Yan, W. Sun, L. Fan, P. N. Duchesne, W. Wang, C. Kübel, D. Wang, S. G. H. Kumar, Y. F. Li, A. Tavasoli, T. E. Wood, D. L. H. Hung, L. Wan, L. Wang, R. Song, J. Guo, I. Gourevich, A. A. Jelle, J. Lu, R. Li, B. D. Hatton, G. A. Ozin, *Nat. Commun.* **2019**, *10*, 2608; c) M. Marwood, R. Doepper, M. Prairie, A. Renken, *Chem. Eng. Sci.* **1994**, *49*, 4801.

[13] a) B. H. Lipshutz, K. Noson, W. Chrisman, A. Lower, *J. Am. Chem. Soc.* **2003**, *125*, 8779; b) C. Jager, T. Welzel, W. Meyer-Zaika, M. Epple, *Magn. Reson. Chem.* **2006**, *44*, 573.

[14] a) J. Y. Y. Loh, N. P. Kherani, G. A. Ozin, *Nat. Sustain.* **2021**, *4*, 466; b) K. K. Ghuman, T. E. Wood, L. B. Hoch, C. A. Mims, G. A. Ozin, C. V. Singha, *Phys. Chem. Chem. Phys.* **2015**, *17*, 14623; c) L. B. Hoch, P. Szymanski, K. K. Ghumanc, L. He, K. Liao, Q. Qiao, L. M. Reyes, Y. Zhu, M. A. El-Sayed, C. V. Singh, G. A. Ozin, *Proc. Natl. Acad. Sci. U. S. A.* **2016**, *50*, 201609374.